HF radars: Physical limitations and recent developments

K.-W. Gurgel [a], H.-H. Essen [a] and S. P. Kingsley [b]

[a] *University of Hamburg, Institute of Oceanography,*
Troplowitzstrasse 7, D-22529 Hamburg, Germany.
Tel: +49-40-4123-5742, Fax: +49-40-4123-5713,
email: gurgel@ifm.uni-hamburg.de
WWW: http://ifmaxp1.ifm.uni-hamburg.de/

[b] *University of Sheffield, Sheffield Centre for Earth Observation Science,*
Department of Electronic and Electrical Engineering,
Mappin Street, Sheffield S1 3JD, UK.
Tel: +44-114-222-5586, Fax: +44-114-272-6391,
email: s.kingley@sheffield.ac.uk

Abstract

High-frequency (HF) radars based on ground-wave propagation are used for remotely sensing ocean surface currents and gravity waves. For some 20 years a number of sytems have been developed taking advantage of improved electronics and computer techniques. However, the performance of these systems are limited by physical constraints, which are due to HF wave propagation and scattering as well as to the technical design of the measuring system. Attenuation of the HF ground-wave is strongly dependent on the radio frequency and sea-water conductivity. Experimental data confirm the predicted decrease of propagation range with decreasing conductivity. HF radar systems use different methods of spatial resolution both in range and azimuth. Range resolution by means of short pulses and frequency-modulated chirps is compared, as well as azimuthal resolution by means of beam forming and direction finding (phase comparison). The emphasis is placed on recent developments.

Key words: HF radar, ground-wave propagation, working range, spatial resolution, beam forming, side lobes.

1 Introduction

Radars, as used by ships or satellite remote sensing, operate in the microwave band with wavelengths of some centimeters, whereas the high-frequency (HF)

band covers frequencies between 3 MHz and 30 MHz with wavelengths of 100 m to 10 m. Due to these large wavelengths, HF radars are not appropriate for operation from satellites. For remotely sensing the ocean HF radars are mostly operated from the coast, except for a few attempts at ship-based operations. Remote sensing by means of HF radar is based on skywave or ground-wave propagation. Refraction by the ionosphere allows large propagation ranges to be achieved. However, the ionosphere undergoes temporal changes and modulates the signal from the sea surface. This paper deals with ground-wave propagation only.

The working range of an HF radar depends on the attenuation of the electromagnetic wave between the transmitter and target and back, the scattering strength of the target, atmospheric noise and noise due to radio interference. Parts of the transmitted HF power propagate along the sea surface following the earth's curvature beyond the horizon. However, this ground-wave is strongly attenuated and in turn the working range is limited. The attenuation increases with increasing HF frequency and decreasing sea-water conductivity. Theoretical dependencies are presented and compared with measurements from areas of different conductivity.

HF remote sensing is based on the scattering of electromagnetic waves from the rough sea surface. As the ocean wave spectrum nearly always contains sea wavelengths of the order of the radar wavelength, the Bragg scattering theory is applicable. In the case of a monostatic configuration, i.e. transmitter and receiver at the same position, first-order Bragg backscattering is due to ocean waves of half of the radar wavelength travelling towards or away from the radar site. Thus, the Doppler spectrum of the backscattered signal contains two lines, the frequencies of which are determined by the phase velocity of the scattering ocean waves. Deviations from the theoretically known values in nonmoving water are attributed to an underlying surface current. The strengths of the Doppler lines reflect the spectral density of the two first-order scattering ocean waves. The full ocean wave spectrum is involved in second-order scattering and generates side-bands in the HF-Doppler spectrum. These can be used for determining, by means of inversion techniques, the two-dimensional wave-height spectrum.

The basic physics of backscattering of electromagnetic waves from a rough moving sea surface was discovered and described by Crombie in 1955 [5]. The first HF remote sensing system for the measuring of surface current was the Coastal Ocean Dynamics Applications Radar (CODAR) developed in 1977 at NOAA by Barrick *et al.* [2]. Based on CODAR, further developments have been made in the UK by Marconi with the Ocean Surface Current Radar (OSCR), cf. Prandle *et al.* [16], in the United States with Barrick's SeaSonde, cf. Paduan and Rosenfeld [14], and in Germany, cf. Gurgel *at al.* [8]. In addition to a great number of land-based experiments, both the CODAR and the OSCR

have been operated from onboard a ship, by Gurgel and Essen [9] and Peters and Skop [15], respectively.

Developments of HF radars, independent of CODAR, have been made in Canada at C-CORE, cf. Hickey *et al.* [12], in the UK at the University of Birmingham, cf. Shearman and Moorhead [17], in France at the University of Toulon, cf. Broche *et al.* [4], in Australia, cf. Heron *et al.* [11], and in Japan, cf. Takeoka *et al.* [19]. There also exist several skywave HF radar systems all over the world, e.g. in France, cf. Sixt *et al.* [18]. Recently, the University of Hamburg developed a new system WERA (Wellen Radar) using FMCW (frequency modulated continuous wave) techniques, cf. Gurgel *et al.* [10], this issue. FMCW is to be distinguished from FMICW (frequency modulated interrupted continuous wave) which was employed in the UK and SeaSonde radars, as discussed below.

2 Working ranges

Working ranges are determined by the signal-to-noise ratio, which in the case of HF remote sensing depends on propagation loss and scattering strength of the rough sea surface.

2.1 HF ground-wave propagation

HF remote sensing of the ocean surface makes use of the ground-wave propagating along the sea surface. This wave is affected by the material parameters of both the sea and atmosphere. The complex (relative) dielectric constant ϵ is given by,

$$\epsilon = \begin{cases} 1 & \text{in the atmosphere,} \\ 80 + \mathrm{i}\sigma/(\epsilon_o\omega) & \text{in water at HF frequencies,} \end{cases} \tag{1}$$

where $\epsilon_o = 8.85 \times 10^{-12}\mathrm{As/Vm}$ is the absolute permittivity in vacuum, σ the conductivity and ω the angular HF frequency. The attenuation of HF propagation depends strongly on the imaginary part of ϵ, i.e. frequency and conductivity. The conductivity σ is a function of salinity and temperature. By using the appropriate formulas, summarized by Dietrich *et al.* [6], these dependencies are displayed in figure 1.

As in the propagation of seismic surface waves, the electromagnetic boundary conditions at the air-sea interface allow cylindric free-wave solutions (Zenneck wave). However, these solutions reveal group-velocities higher than the speed

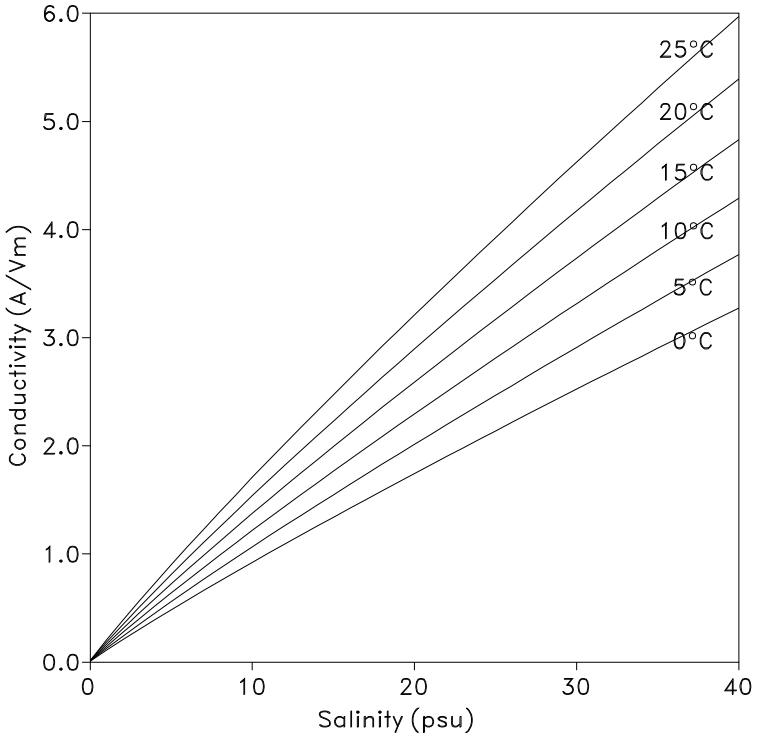

Figure 1. Conductivity of sea water as function of salinity at six different temperatures.

of light and do not correspond to real waves. The field of a vertical electric dipole of constant frequency has been evaluated by Wait [20] by means of the saddle point method. The solution for any electromagnetic field variable can be written as,

$$\psi(r,t) = \frac{1}{r} A(\omega, \sigma, r) \exp[\mathrm{i}\omega(\frac{r}{c} - t)], \tag{2}$$

where r is the distance between transmitter and receiver, t the time and A an attenuation factor. This solution predicts a spherical rather than the cylindric attenuation of surface waves, which additionally is increased by an attenuation factor. Figure 2 demonstrates the dependencies of attenuation on frequency and conductivity. The numerical results refer to a plane earth with both transmitter and receiver located at the sea surface.

Figure 3 displays the attenuation of HF waves over sea, measured over different areas of water. In each case the transmit antenna was installed on shore, the receive antenna onboard a ship or on a sledge. Continuous wave (CW) signals of either 25.4 MHz or 29.85 MHz have been transmitted and recorded during stops. An intercomparison of the measurements from different sites and with theoretical results requires some caution. The antenna setups were different, antenna gains are not accounted for and neither are coupling losses between antennas and sea surface. The two frequencies used in the North Sea

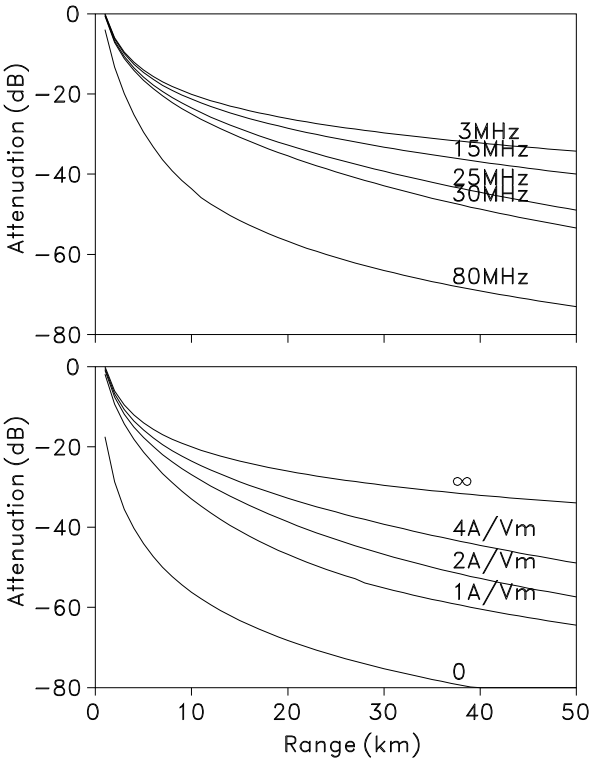

Figure 2. Theoretical HF attenuation (arbitrarily normalized) over a plane ocean. Upper panel: in terms of frequency at a conductivity of 4 A/Vm (ocean water, cf. figure 1), lower panel: in terms of conductivity at a frequency of 25 MHz.

show no significant difference. However, the dependence of the attenuation on the conductivity becomes clearly visible and confirms the theoretical results of figure 2. Due to the high attenuation, the attempt of measuring surface currents by means of HF failed in the fresh-water lake. On the other hand, current measurements in the highly salty Dead Sea could be performed with extremely low transmit power, cf. Essen *et al.* [7].

2.2 Backscatter from the rough sea surface

As is generally accepted, resonant Bragg scattering is the dominant process generating HF radar backscatter. The weak nonlinear interaction between the incident electromagnetic wave and the gravity sea surface wave field generates scattered electromagnetic waves, which partly return to the radar site. The first-order theory predicts two discrete lines for the backscattered Doppler spectrum f_1,

$$f_1(\omega_d) = \sum_{s=\pm 1} T_1 F(\mathbf{k}_B)\delta(\omega_d - s\omega_B), \quad \mathbf{k}_B = -2s\mathbf{k}_o, \tag{3}$$

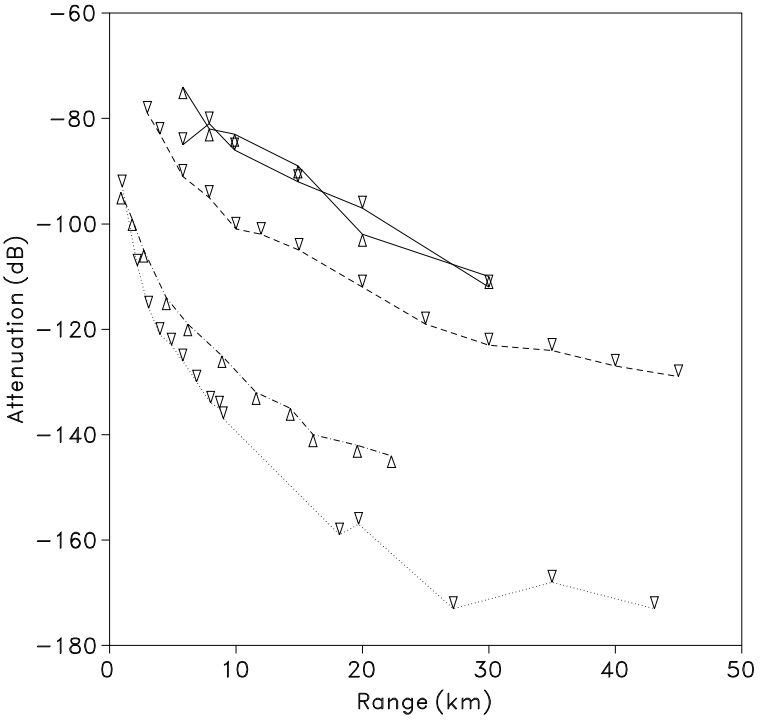

Figure 3. Measured HF attenuation at different sites. Full lines: North Sea (σ = 4.0 A/Vm), dashed line: Baltic (σ = 1.5 A/Vm), dashed-dotted line: fresh-water lake, dotted line: ice. The transmit frequencies are 25.25 MHz ($\bigtriangledown$) and 29.85 MHz ($\bigtriangleup$).

where ω_d is the Doppler frequency, $\mathbf{k}_o$ the HF wavevector, ω_B and $\mathbf{k}_B$ are the frequency and wavevector of the Bragg scattering surface waves, which propagate towards or away from the radar site. $F(\mathbf{k})$ is the two-dimensional spectral density of the surface wave heights. The transfer function T_1 depends on frequency and polarisation of both transmitter and receiver. It also accounts for the attenuation between the scattering patch and the radar site. HF ground-wave remote sensing is based on scattering at grazing incidence. In a recent paper, Barrick [3] points out that in this case propagation and scattering become interrelated, and plane waves are inadequate to represent radiation from sources in the region very near or below the horizon. I.e. theoretical transfer functions, derived for plane waves and a perfectly conducting sea, have to be considered with caution.

Considering HF radars with frequencies of some 30 MHz, the wavelengths of the order of 10 m are, in general, smaller than the dominant open ocean surface waves ($\approx 100m$). For this case, the second-order HF Doppler spectrum f_2 can be represented by,

$$f_2(\omega_d) = \sum_{s,s'=\pm 1} F(\mathbf{k}_B) \int T_2 F(\mathbf{K}) d\varphi, \quad \omega_d = s\omega_B + s'\Omega, \tag{4}$$

where the frequency Ω and wavevector $\mathbf{K} = (\Omega/c)[\sin\varphi, \cos\varphi]$ refer to the dominant long waves of the spectrum. T_2 is a transfer function with dependencies similar to T_1. In contrast to the first-order Doppler spectrum, the second-order spectrum is continuous. It contains information on the long-wave ocean spectrum. It should be mentioned that Eqs. (3-4) are derived by means of a perturbation expansion, which is based on the assumption that the surface wave amplitudes are much smaller than the HF wavelength.

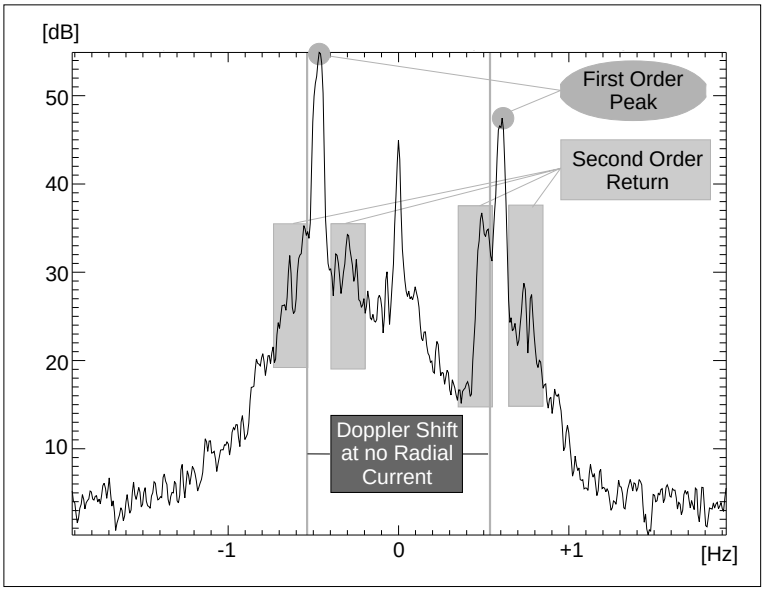

Figure 4. Measured HF Doppler spectrum. First-order lines and second-order side bands are indicated.

Figure 4 displays a measured Doppler spectrum, received from a limited patch of the sea surface. Due to an underlying current the two first-order peaks are displaced from the theoretical lines by the same amount, which is proportional to the radial current speed. The second-order side bands are indicated.

2.3 Working ranges of current measurements

Data presented here are from an experiment at the Dutch coast performed in 1996 with two WERA radar sites some 10 km apart. The transmit frequency was 27.65 MHz, and the systems were operated with linear arrays of receive antennas. Details about the WERA system and the experiment are given by Gurgel *et al.* [10], this issue. The experiment lasted six weeks during which the weather underwent strong changes. The scattering Bragg wavelength (half the radar wavelength) is 5.4 m and strongly affected by local winds. Because of Eq. (3) it may be expected that the working range increases with increasing wind waves. However, experimental data reveal the opposite effect.

Figure 5 displays the backscattered signal strengths as function of range for

measurements during low and high sea states. The signal strength contains the power of both first order lines in figure 4 and is an average over all beams from -60^o to +60^o around boresight of the antenna array. I.e. the signal strength presented is an integral over the directional distribution of surface waves. As a reference, the noise level is plotted, which is the mean power from the edges of the spectrum in figure 4. This noise is independent of sea-state. Obviously the system's internal noise masks the atmospheric and scattering noise. At near ranges higher waves cause higher signal strength, which is in accordance with Eq. (3). However, at intermediate ranges the opposite is the case, which means that the working range decreases with increasing sea state. This finding is in accordance with theoretical investigations by Barrick [1] (1971). At far ranges the power curve of the high sea-state becomes unstable, most probably due to noise induced by other processes than Bragg scattering, e.g. shadowing effects or absorption by foam.

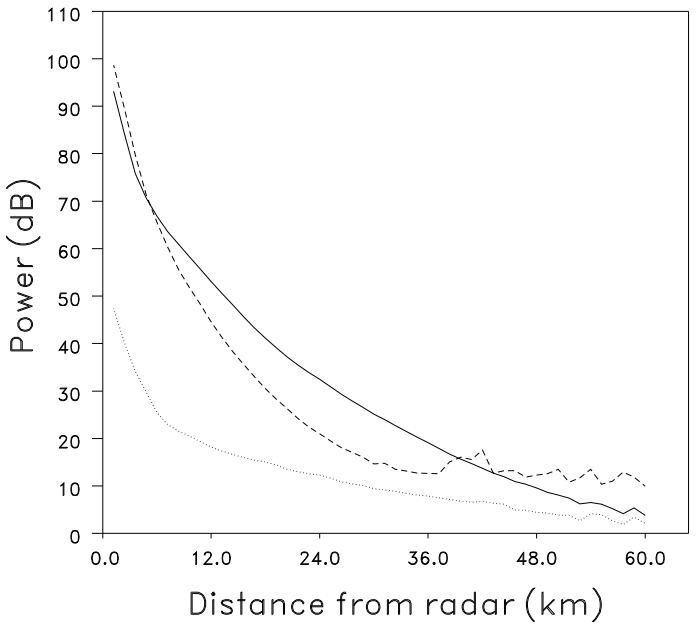

Figure 5. Signal strength versus range, as measured by the HF radar WERA. Full lines refer to a mean wave height of $H_{1/3}$ = 60 cm, dashed lines to $H_{1/3}$ = 400 cm. Dotted line displays the system's internal noise which is independent of sea state.

Two-dimensional surface currents are composed on a given grid from radial components measured by two radar stations. A surface current vector is established if the first-order Bragg lines of both stations exceed the noise level by a certain amount. For further investigating the dependence of working range on sea state, figure 6 displays the area covered by current-vectors found in terms of the significant waveheight as measured by a wave buoy in the measuring area. Defining the square root of the covered area as working range, it can be stated that the working range decreases from 45 km at a significant waveheight

of 50 cm to 22 km at 400 cm waveheight. This finding does not necessarily contradict Eq. (3) because the significant wave height is determined by waves longer than the Bragg wave. However, it is not likely that the amplitude of the Bragg wave decreases with increasing significant waveheight.

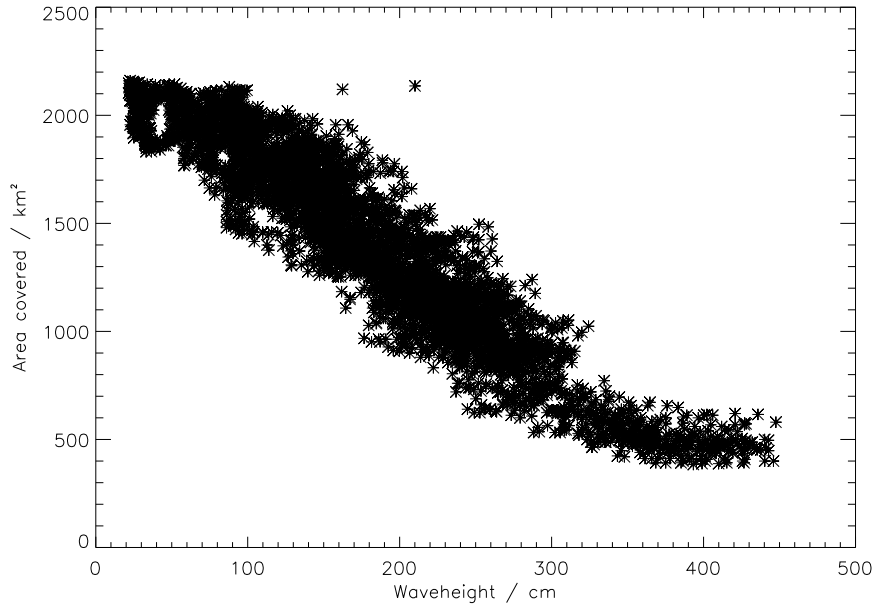

Figure 6. Area covered by two separate HF radars as function of mean waveheight ($H_{1/3}$). Coverage of a grid patch is established if both radars reveal a significant first-order signal.

Most probable reasons for the decrease of working range with increasing sea state are: 1) scattering losses in addition to the attenuation on the propagation path, and 2) distortion of the linear scattering field due to wave breaking and foam.

3 Limitations of spatial resolution

For the purpose of remote sensing, an HF radar system has to perform spatial resolution both in range and azimuth. Range resolution is limited by two requirements. The scattering range has to extend over a large number of HF wavelengths in order to allow resonant backscatter. The disturbance by radio interference has to be minimized by using transmit signals of narrow bandwidth and in turn coarse range resolution. This latter problem is especially acute with low-frequency HF radars. For both the requirements mentioned, the possible range resolution decreases with decreasing frequency, i.e. a compromise has to be found between range resolution and working range, which increases with decreasing frequency.

Long range HF radio transmission makes use of waves, which travel to a distant point by repeated back-and-forth reflection from the ionosphere and the earth. There is an upper limit to HF frequencies that are reflected by the ionosphere, which is called the maximum usable frequency (MUF). The MUF is highest near noon or in the early afternoon and is highest during periods of greatest sunspot activity, cf. Orr [13]. The MUF can drop to 5 MHz or go up to 30 MHz. HF radars working with frequencies below the MUF are strongly affected by interference with radio transmission from all over the world. They have to operate with a narrow bandwidth in order to realize a suffcient signal-to-noise ratio. For example, at a transmit frequency of 6 MHz the bandwidth should not exceed 20 kHz, which corresponds to a range resolution of 7.5 km. This distance is 150 times the HF wavelength of 50 m.

Frequencies in the upper HF band, e.g. between 25 MHz and 30 MHz, allow an increased range resolution. At these frequencies a bandwidth of up to 500 kHz is possible corresponding to a range resolution of 0.3 km. However, during periods of high sunspot activity the MUF can exceed 25 MHz. Then, higher transmit frequencies around 30 MHz should be selected, in spite of the increase in attenuation. For this reason, the CODAR of the University of Hamburg has been operated at 29.85 MHz, cf. Gurgel *et al.* [8]. The sunspot activity varies with a period of 11 years and is increasing at the moment.

Table 1
Working range for current measurement and range resolution of existing HF-radars in dependence of transmit frequency. Working range for wave measurements is less because of more severe signal-to-noise requirements.

Operating frequency		Working range	Frequency bandwidth	Range resolution	Antenna size	Radio interference
6.75 MHz	[12]	200 km	20 kHz	7.5 km	≈870 m	very high
7 MHz	[17]	200 km	20 kHz	7.5 km	≈200 m	very high
25 MHz	[2,19]	60 km	125 kHz	1.2 km	≈90 m	variable
27 MHz	[10]	40 km	500 kHz	0.3 km	≈83 m	low
27 MHz	[10]	55 km	125 kHz	1.2 km	≈83 m	low
30 MHz	[8]	50 km	125 kHz	1.2 km	≈75 m	low
55 MHz	[15]	15 km	600 kHz	0.25 km	≈83 m	low

There is no interference from long range radio sources with VHF frequencies higher than 50 MHz. Disturbances can only arise from near-by radio stations. Broad bandwidths can be used to realize high spatial resolutions. However, the working range at these frequencies is strongly reduced because of the high attenuation of the HF ground-wave, cf. figure 2. Table 1 summarizes the specifications of existing HF radar systems. The data refer to a non-directional

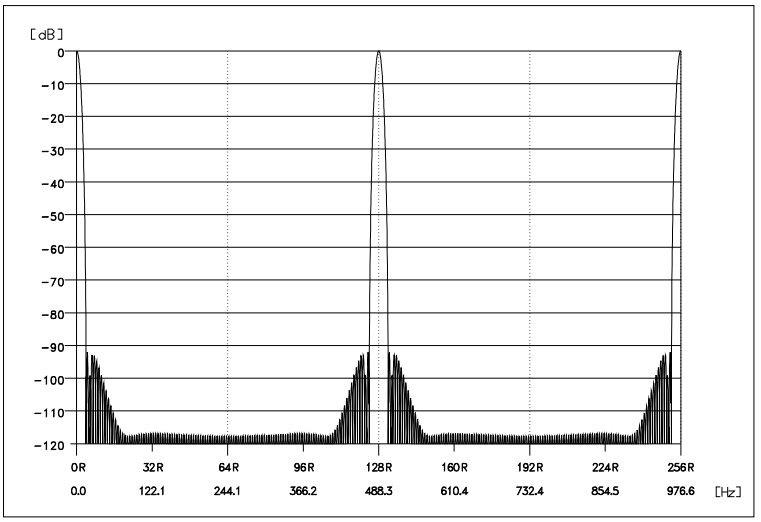

Figure 7. Filter function of 128 CODAR samples, weighted by a Blackmann-Harris window.

transmit antenna and sea water of 35 psu. The antenna size presented is the extent of a linear array of receive antennas, though some of the systems referred to make use of other configurations (see below).

3.1 Techniques of range resolution

Different techniques for range resolution are possible and are used by the HF radars mentioned. The main techniques are the transmission of either CW pulses or linear FMCW chirps. The physical principles are discussed by Gurgel *et al.* [10], this issue, whereas the following presentation is focused on technical problems. The advantage of range resolution by CW pulses is the simple design. Disadvantages are the high peak power needed and a high noise level due to aliasing. These problems are discussed with respect to the CODAR system, which is connected to four receive antennas (see below).

The CODAR of the University of Hamburg, cf. Gurgel *et al.* [8], transmits tapered CW pulses with an effective duration of about 13 μs, the repeat period is 512 μs. Multiplexing of the four receive antennas reveals a repetition cycle of 2048 μs for each antenna. Most of the time is needed for receiving and only little time ($\approx$ 2.5% duty cycle) used for transmitting. In order to realize the working ranges of Table 1 the pulses have to be transmitted with high power, which however is limited for technical and safety reasons to about 10 kW. In most experiments the CODAR has been operated with a peak power of 3 kW, which corresponds to an average power of less than 80 W.

The received CODAR signal is phase-coherently demodulated, A/D converted and sampled into range cells. In order to obtain a sampling rate which is ap-

propriate for sea-surface variability, 128 samples are averaged. The resulting sampling rate is 0.262 s, which corresponds to bounds of ± 1.9 Hz of the Doppler spectrum. However, the Doppler spectrum accounts not only for frequencies of ± 1.9 Hz around the HF carrier, but due to aliasing for a much broader band. To some extent aliasing is suppressed by applying a Blackman-Harris window. However, there are passbands at multiples of ± 128 × R, where R = 3.8 Hz is the width of the Doppler spectrum. Figure 7 displays the filter function for positive frequencies relative to the HF carrier. The bandwidth of the transmitted signal is 125 kHz, i.e. the 256 passbands fold back into the signal band. Even if they contain no radio signal, their noise significantly reduces the signal-to-noise ratio (by 24 dB for the CODAR). This is a principle problem for HF radar systems performing range resolution by means of CW pulses. The number of samples available for averaging decreases with the number of multiplexed antennas, and in turn the noise level increases (to 30 dB for the OSCR with 16 antennas).

The FMCW technique avoids the aliasing problem discussed. Further advantages are the possibility of simply altering the range cell depth by means of the chirp width. It also turns out that FMCW techniques are more robust against radio interference. On the other hand, the transmitter and receiver must be designed for extreme dynamic range and linearity. High energy signals from near ranges and low energy signals from far ranges are superimposed and have to be processed simultaneously and separated to resolve ranges. In order to reduce dynamic range requirements, FMICW (frequency modulated interrupted continuous wave) techniques can be applied, which requires some transmit/receive switching. However, this method does not avoid the blind range in front of the radar. For some applications the coverage of this near-coastal zone is important.

The frequency of a chirp increases linearly with time, cf. Gurgel *et al.* [10], this issue,

$$f(t) = f_o + \frac{b}{T}t, \quad 0 \leq t < T, \tag{5}$$

where f_o is the transmit frequency. The frequency width b determines the range resolution, and the chirp length T the sampling rate of the sea surface, which for WERA is $T = 0.26$s, i.e. about the same as for CODAR. The chirps are phase-continuously repeated. Range resolution is performed by Fourier analysing the response of each single chirp. The procedure is strongly affected by the leakage problem. Figure 8 displays the result of a simulation study. The analysed signal has been synthesized by considering two moving targets of ± 0.5 Hz Doppler shift in the first range cell, which corresponds to first-order Bragg scattering from ocean waves. The spectral densities refer to the application of no window to the time series, a Blackman-Harris window and

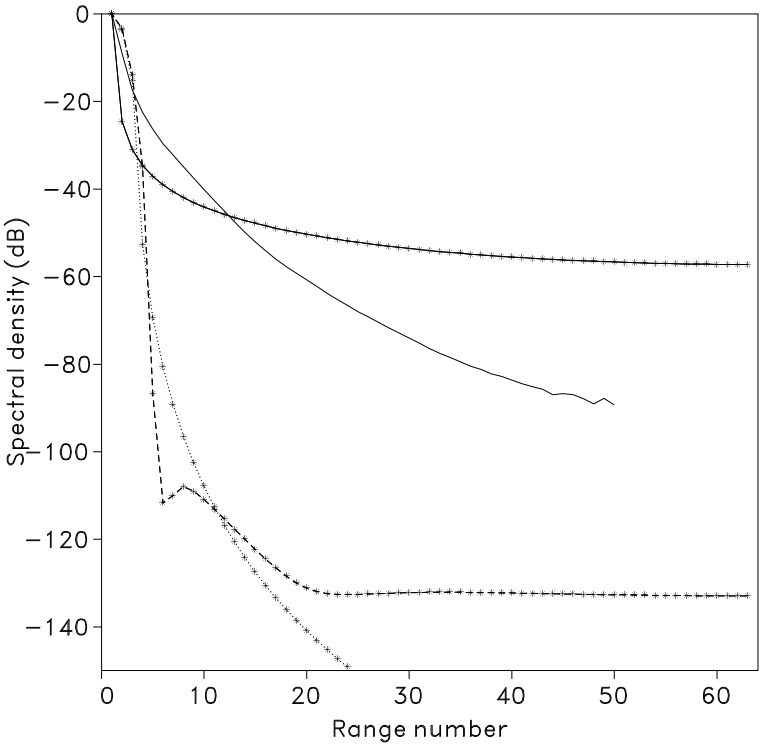

Figure 8. Spectral density of a synthesized chirp, applying no window (solid line with stars), a Blackman-Haris window (dashed line with stars) and a $\cos^4$-window (dotted line with stars). The solid line reproduces the measured signal strength of figure 5.

a $\cos^4$-window. The Blackman-Harris window is applied by WERA. The $\cos^4$-window reveals even higher suppression of far ranges, but reveals a less steep decrease for near ranges. The full line reproduces the experimental decrease of signal strength of a 27.75 MHz WERA measurement under low wind condition (figure 5). The curves demonstrate that windowing is essential for resolving the low-power far-range signals. Windowing however, causes some overlap of the samples of adjacent range cells.

3.2 Techniques of azimuthal resolution

Two methods of azimuthal resolution will be discussed, direction finding and beam forming. In both cases it is assumed that the transmit antenna is omnidirectional or slightly directed towards the sea, and azimuthal resolution performed by means of an array of receive antennas. Each single antenna receives echoes from different azimuthal directions which are superimposed.

Direction finding is based on the Fourier decomposition of the time series received by three or four antennas. Each Fourier line is attributed to a Doppler shift and in turn to a radial speed. It is assumed that the different radial speeds

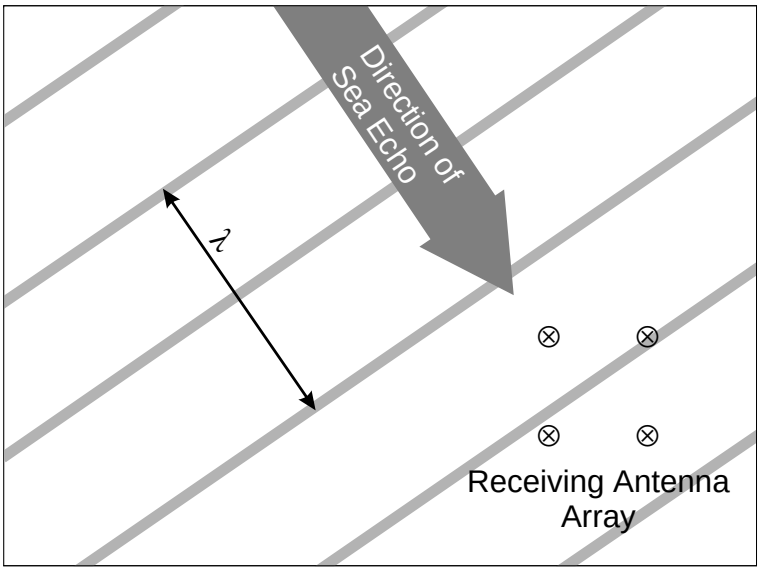

Figure 9. Principle of direction finding. The diagonal of the square antenna array is 1/2 of the electromagnetic wavelength λ.

arrive from different directions, which are determined by comparing the amplitudes and phases at the receive antennas. Figure 9 illustrates the principle of direction finding for a single plane wave, i.e. one Fourier component. In order to avoid ambiguities, the diagonal of the antenna array must be equal or less than one half of the electromagnetic wavelength. Some further information on direction finding algorithms is presented in the papers of Gurgel *et al.* [9,10].

The main advantage of direction finding is the small size of the array of receive antennas. Direction finding has been applied successfully for surface current measurements in some 15 field experiments by the CODAR of the Univerisity of Hamburg. The main disadvantage of direction finding is that it is not appropriate for extracting information on the sea state. The second-order signal from a certain direction is masked by first-order signals from deviating directions. Another disadvantage is the assumption that the different radial velocities all come from different directions, which might be invalid in a very inhomogeneous current field. Subdividing the timeseries in overlaping parts and sophisticated algorithms help to overcome this limitation, however beam forming does not depend on such an assumption.

An alternative way to gain directional information on currents, and additionally on waves, is to form a set of real narrow beams. Large antenna arrays are needed to do this, which can be both expensive and cause siting problems. The output of a linear array of several antennas (typically 16) can be combined, in a process known as beamforming, to make narrow beams which are generally limited to a minimum width of about λ/D radians where λ is the radar wavelength and D is the overall length of the array. The optimum distance of adjacent antennas is $\lambda/2$.

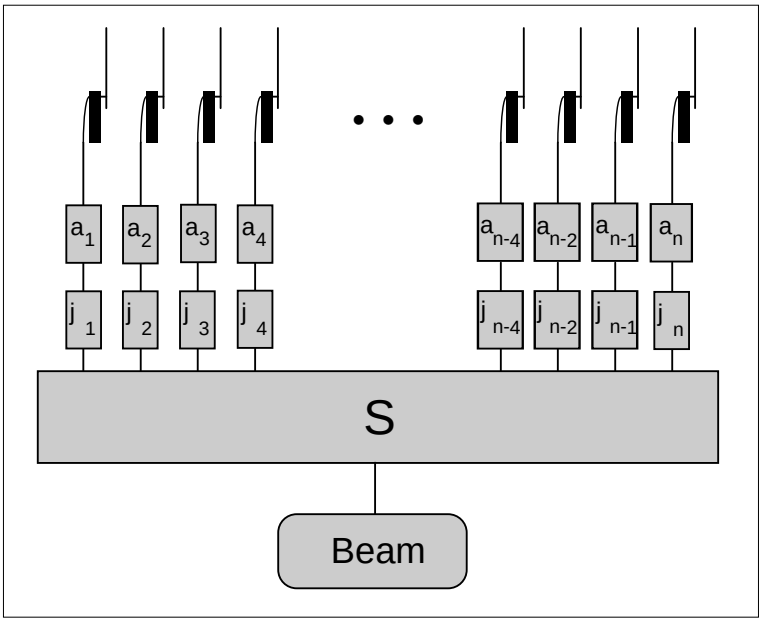

Figure 10. Principle of beamforming. After weighting by a_i and phase shifting by φ_i the signals of n receive antennas are added.

The advantage of beamforming is that the beams can be steered to achieve a particular area coverage which may be localised around a buoy, for example, or which might be a wide area of ocean. Beamforming generally increases the antenna gain which in turn increases the signal-to-noise ratio of the echoes received. Modern digital beamformers can also be configured to form nulls in the antenna pattern in the direction of any interfering radio systems.

The oldest types of beamformers make use of time delays in cables. If all the cables from the antennas to the receiver are the same length then a beam is formed along the boresight perpendicular to the array. By introducing a progressive increase in cable length from one end of the array to the other the beam can be steered to either side of boresight as required, up to a practical maximum of perhaps 45 degrees. These time delay beamformers are slow and unreliable but have the great advantage of having a very wide instantaneous bandwidth.

At any given spot frequency the effect of a time delay at each antenna can be reproduced by electronically inserting the equivalent phase change. It is much quicker to steer a beam using such phase beamsteering and the unreliability, expense and weight of cables and switches can be avoided. There are many ways of electronically changing the phase of a radio signal and the only real disadvantage of these systems, the limited instantaneous bandwidth, is not usually a problem for HF radar sea-sensing.

The most advanced type of forming antenna patterns is digital beamforming. Here each antenna element in the array has its own receiver and A/D converter

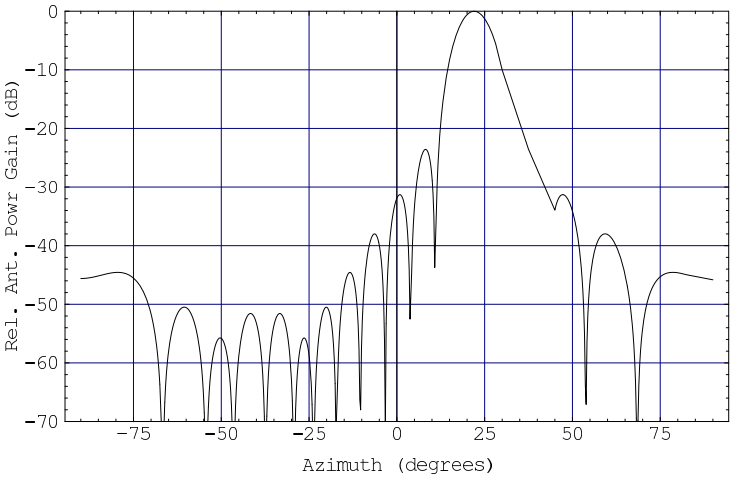

Figure 11. The theoretical antenna pattern of a 16 element array when the beam is steered 22^o off boresite. Cosine weighting has been applied in this case.

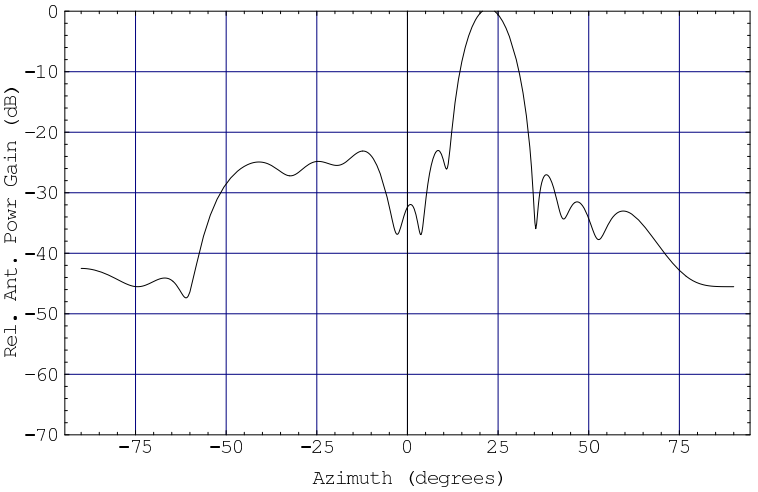

Figure 12. As above, but the pattern when the antenna is installed on real ground at an angle to the coastline.

and beams are formed by digitally processing all the outputs. The system is very flexible and beams can be recalculated to any shape and even formed after the experiment. Different weighting (window) functions can be applied to control the antenna sidelobes and correction factors can be built in to account for the end elements of the array behaving in a different way to those at the centre. The WERA radar of Gurgel *et al.* [10] uses this type of beamforming, as shown in figure 10.

One problem affecting most long linear arrays is the problem of erecting them on a straight coastline. When two radars are used to survey an area of water then the two arrays must either be erected parallel to the shoreline, in which case their beams barely intersect, or they must be installed at an angle to the coast. In this latter case, antenna elements at one end of the array must

necessarily be erected closer to the sea than those at the other. The differential radio propagation along land/sea paths is so great that the beams formed have much higher sidelobes than desired. Figure 11 shows a typical idealised beam formed from a 16 element array parallel to the coast and figure 12 shows the pattern of the same array when set at an angle to a real coastline. Again, this does not usually create problems when measuring currents but it can cause corruption of some wave measurements. There is really no easy way round this problem, but the more compact the antenna array can be made the smaller the effect and it is now generally recognised that there is a need to develop such arrays.

3.3 Operational HF radar systems

Table 2
Range- and azimuthal resolution of existing HF radar systems as well as the illumination by the transmit antenna (wide angle or narrow beam).

System	Pulse	FM(I)CW	Transmit **w**ide/**b**eam	Direction finding	Beam forming
CODAR / NOAA [2]	X		w	X	
OSCR [16]	X		w		X
PISCES [17]		(I)	w		X
C-CORE [12]		(I)	w		X
COSRAD [11]	X		b		X
SeaSonde [14]		(I)	w	X	
WERA [10]		X	w	X	X

Table 2 summarizes the techniques as applied by HF radar systems presented in the literature. Respective working ranges and range resolution are listed in Table 1. The original CODAR developed at NOAA performes range resolution by means of pulses and uses the 4-element square array as shown in figure 9 with direction finding for azimuthal resolution. The OSCR makes use of a linear array and beam forming as shown in figure 10. The PISCES radar is based on FMICW modulation for range resolution and beam forming provided in hardware by switchable cables used as phase shifters. FMICW introduces transmit / receive switching to overcome dynamic range limitations. The C-CORE Cape Race system provides a high azimuthal resolution by a 40-element linear array, which is some 1 km long. This is a very large permanent installation for research, i. e. tracking icebergs. The Australian COSRAD radar (Coastal Ocean Surface Radar) developed at James Cook Univerisity is operated at 30 MHz and uses pulses of 20 μs duration which yield 3 km range

resolution. In contrast to the other systems mentioned, which perform illumination of the measurement area by a wide angle transmit antenna, a common antenna array for transmit and receive is used to perform beam forming. This has the advantage of squared sidelobe directivity performing a narrower beam and increases the signal-to-noise ratio. However, as the different directions are scanned step by step, the azimuthal surveillance is slow and technical problems in switching the antenna between transmitter and receiver arise. The SeaSonde is a very small portable system using FMICW for range resolution. Azimuthal resolution is provided by a very small loop antenna combined with a special direction finding algorithm different from the one described in this paper. Finally, WERA uses FMCW (without transmit / receive switching) for range resolution and beam forming or direction finding techniques for azimuthal resolution as described in this paper, depending on the application's requirements.

4 Conclusions

Working ranges of ground-wave based HF radar systems are strongly dependent on transmit frequency and sea-water conductivity. High salinity allows optimum performance, while strong attenuation prevents HF radars being used for remote sensing in fresh-water lakes and over ice covered areas. Considering typical oceanic water, working ranges of more than 100 km are possible with HF frequencies of 6 MHz. However, the resolution is limited to some 8 km. Higher frequencies allow finer resolution, e.g. 0.3 km with HF frequency of 30 MHz. In this case, the working range decreases to less than 50 km.

HF radar systems apply different methods for spatial resolution, both in range and azimuth. Range resolution by means of frequency modulated continuous wave (FMCW) chirps requires a more advanced technique than the resolution by means of continuous wave (CW) pulses. However, the FMCW method is advantageous in several aspects. It allows more flexibility in altering transmit frequency and range resolution. In principal, the signal-to-noise ratio can be improved by avoiding aliasing problems and it should be possible to increase the presently realized working range. The main advantage of performing azimuthal resolution by means of direction finding is the small extend of the receive antenna array, i.e. $\approx 1/2$ electromagnetic wavelength. However, this configuration is appropriate for current measurements only. The reliable estimation of surface-wave spectra requires azimuthal resolution by means of beamforming, i.e. the installation of a linear receive antenna array with an overall length of ≈ 8 electromagnetic wavelengths.

Acknowledgements

This work was partly funded by the EC (DG XII, MAST-II, MAS2-CT94-0103) within SCAWVEX. We wish to thank the other members of the University of Hamburg HF-radar group, Florian Schirmer, Thomas Schlick and our technician Monika Hamann for supporting the measurement campaigns, developing algorithms and processing data, and the Dutch Rijkswaterstaat, H. C. Peters, J. Vogelzang, A. Wijzes and local authorities for excellently supporting the logistics and supplying topographic and oceanographic data.

References

[1] D. E. Barrick, Theory of HF and VHF propagation across the rough sea, 2, Application to HF and VHF propagation above the sea, *Radio Science* **6** (1971) 527–533.

[2] D. E. Barrick, Ocean surface current mapped by radar, *Science* **198** (1977) 138–144.

[3] D. E. Barrick, Grazing behaviour of scatter and propagation above any rough surface, *IEEE Transactions on Antennas and Propagation* **46** (1998) 73–83.

[4] P. Broche, J. C. Crochet, J. L. de Maistre, and P. Forget, VHF radar for ocean surface current and sea state remote sensing, *Radio Science* **22** (1987) 69–75.

[5] D. D. Crombie, Doppler spectrum of sea echo at 13.56 Mc/s, *Nature* **175** (1955) 681–682.

[6] G. Dietrich, K. Kalle, W. Krauss and G. Siedler, Allgemeine Meereskunde (3. Aufl.), *Gebrüder Borntraeger*, Berlin (1975).

[7] H.-H. Essen, K.-W. Gurgel, F. Schirmer and Z. Sirkes, Horizontal variability of surface currents in the Dead Sea. *Oceanologica Acta* **18** (1995) 455–467.

[8] K.-W. Gurgel, H.-H. Essen and F. Schirmer, CODAR in Germany - a status report valid November 1985 -, *IEEE J. Oceanic Engineering*, **11** (1986) 251-257.

[9] K.-W. Gurgel and H.-H. Essen, On the performance of a ship-borne current mapping HF radar, *IEEE Oceanic Engineering* (1998) submitted.

[10] K.-W. Gurgel, G. Antonischki, H.-H. Essen and T. Schlick, Wellen Radar (WERA), a new ground-wave based HF radar for ocean remote sensing, *Coastal Engineering* (1998) submitted.

[11] M. L. Heron, P. E. Dexter, and B. T. McGann, Parameters of the air-sea interface by high-frequency ground-wave HF Doppler radar, *Aust. J. Mar. Freshwater Res.* **36** (1985) 655–670.

[12] K. Hickey, R. H. Khan and J. Walsh, Parametric estimation of ocean surface currents with HF radar, *IEEE J. Oceanic Engineering* **20** (1995) 139-144.

[13] W. I. Orr, Radio Handbook, 21. edition, *Editors and Engineers*, Indianapoplis (1978).

[14] J. D. Paduan and L. K. Rosenfeld, Remotely sensed surface currents in Monterey Bay from shore-based HF radar (Coastal Ocean Dynamics Application Radar), *J. Geophys. Res.* **101** (1996) 20669–20686.

[15] N. J. Peters and R. A. Skop, Measurements of Ocean Surface Currents from a Moving Ship Using VHF Radar, *Journal of Atmospheric and Oceanic Technology* **14** (1997) 676–694.

[16] D. Prandle, S. G. Loch and R. Player, Tidal Flow through the Straits of Dover, *Journal of Physical Oceanography* **23** (1992) 23–37.

[17] E. D. R. Shearman, M. D. Moorhead, PISCES: A Coastal Ground-wave HF radar for Current, Wind and Wave Mapping to 200 km Ranges, *Proceedings IGARSS'88* (1988) 773–776.

[18] M. Sixt, J. Parent, A. Bourdillon and J. Delloue, A New Multibeam Receiving Equipment for the Valensole Skywave HF Radar: Description and Applications, *IEEE Transactions on Geoscience and Remote Sensing* **34** (1996) 708–719.

[19] H. Takeoka, Y. Tanaka, Y. Ohno, Y. Hisaki, A. Nadai, and H. Kuroiwa, Observation of the Kyucho in the Bungo Channel by HF radar, *Journal of Oceanography* **51** (1995), 699–711.

[20] J. R. Wait, Electromagnetic waves in stratified media, *Pergamon Press*, New York (1962).